STATISTICAL MODELING OF MULTI-DIMENSIONAL FIELDS

Anamarija Borštnik Bračič, Edvard Govekar, Igor Grabec

University of Ljubljana, Faculty of Mechanical Engineering
SI-1000 Ljubljana, Aškerčeva 6, Slovenia

anamarija.bracic@fs.uni-lj.si (Anamarija Borštnik Bračič)

Abstract

An efficient control of laser welding process requires a reliable prediction of process behavior. For this purpose representative variables have to be chosen, which can effectively describe the welding process. Our prediction is based on a record of surface optical activity in the heated zone, known as the melt pool. The spatiotemporal dynamics of surface optical activity is successfully predicted using non-parametric statistical modeling, which is based on assumption that statistical properties of deterministic chaotic fields remain unchanged as the field evolutes with time. An analysis of field patterns in the past enables us to extract relations between values of field in neighboring points in space as well as in time. Based on similarities between the present field pattern and field patterns extracted from the past data, the field value in the next time step can be successfully predicted. In this presentation we show how to optimize field pattern sampling in order to maximize prediction quality. A special attention is paid to the structure of sample vectors, which represent the bridge between the past and the future field distributions. Presented time prediction method, which was applied to the surface optical activity in the heated zone, represents the first step towards the optimal control of laser welding process.

Keywords: Nonlinear dynamics, control, prediction, spatiotemporal data analysis.

Presenting Author's Biography

Anamarija Borštnik Bračič obtained her Ph.D. in Physics at University of Ljubljana. She investigated properties of confined liquid crystals at temperatures above the nematic-isotropic phase transition, which are partially ordered due to the influence of the surface. The research was carried out in collaboration with Institute for theoretical and applied physics at University of Stuttgart. Later on she became involved in research and development projects in the field of industrial automation. She was a leader of automation projects in automobile industry (DaimlerChrylser) and industry of porous concrete building material (Xella). Lately, Anamarija Borštnik Bračič became a member of Laboratory of Sinergetics at Faculty of Mechanical Engineering. Her research is focused to statistical modeling and prediction of time evolution of multi-dimensional fields.

1 Introduction

In order to use laser system as a high performance welding tool, efficient control should be established [1]. The crucial task in planning the control system is to determine representative variables which can effectively describe the welding process. In addition to measurements of intensity and spatial distribution of reflected light or surface temperature, characteristic dynamic properties in space and time can also be obtained by recording surface optical activity in the heated zone, known as the melt pool [2].

After choosing the representative variables, evolution laws have to be extracted from temporal data. To date, this problem has been extensively studied in relation to chaotic time series prediction [3, 4, 5, 6, 7]. The basis of these methods is to reconstruct a state-space from a recorded scalar time series by using an embedded technique, and then to estimate deterministic dynamic evolution from the reconstructed trajectory using statistical average estimators. We present a generalization of this approach, where the modeling of dynamic laws is extended from one dimension (time) to multiple dimensions in spatiotemporal space. This generalization requires a new embedding method, which makes feasible a reconstruction of trajectory in the state-space from spatiotemporal data. The embedded technique, which was initially developed for time series analysis, can be simply generalized to spatially related data [8, 9, 10, 11, 12] and results in a good agreement between predicted and original chaotic fields over short time scales. Since, in a properly reconstructed state-space, the modeled dynamics must have similar statistical properties to the actual dynamics, we use a new state-space reconstruction method which also considers statistical properties of a field structure. Such reconstruction results in an accurate short-term prediction as well as a statistically proper long-term prediction of deterministic chaotic field evolution [13].

The basic motivation of this article is to develop a method for modeling spatio-temporal fields, which could provide for an efficient control of laser welding process. Result shown in this article present a first step in this direction.

In the presented work a statistical method of field generators is used to model the spatiotemporal dynamics of laser welding melt pool images [14]. The stochastic field evolution is modeled from sample state vectors reconstructed from recorded spatiotemporal data. The field evolution equation is estimated non-parametrically from the samples, using the conditional average estimator which determines the governing equation of *radial basis function neural network*. Our goal is to find an optimal dimensionality of the neural network, *i.e.*, to determine its optimal structure and an adequate number of sampling patterns, which will result in the best quality Q of field generator prediction.

Accurate modeling of laser welding images, together with a criterion function specified by the operator of the laser system, provides the basis for optimal control of the laser welding process.

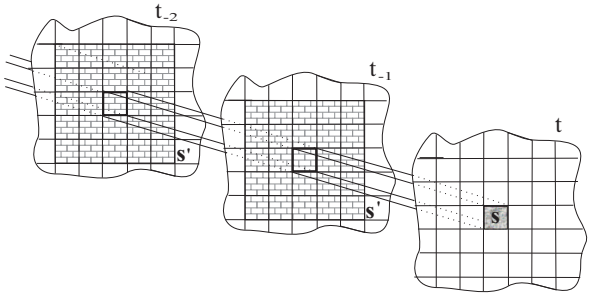

Fig. 1 Illustration of point $\mathbf{s}$ and its surroundings $\mathbf{s}' \in \mathcal{S}$. The future distribution of field φ $(\mathbf{s})$ is located in plane t, while the surrounding points $\mathbf{s}' \in \mathcal{S}$, which represent the past distribution of field, are located in *planes* t_{-1}, t_{-2}...

2 Description of method

2.1 Non parametric statistical modeling

In our model, field evolution is expressed only in terms of data recorded at equally spaced discrete points in space and time, $\varphi = \varphi(\mathbf{s})$, where the variable $\mathbf{s}$ represents space as well as time components $\mathbf{s} = \mathbf{s}(\mathbf{r},\mathrm{t})$. We assume that the dynamics of the field can be described in terms of the generator equation

$$\varphi(\mathbf{s}) = \mathcal{G}\left(\varphi(\mathbf{s}' \in \mathcal{S}(\mathbf{s})), \sigma\right), \tag{1}$$

where $\varphi(\mathbf{s}' \in \mathcal{S})$ represents the *past distribution* of the record, while $\varphi(\mathbf{s})$ represents its *future distribution*. $\mathcal{S}$ represents the surroundings of point $\mathbf{s}$. The field generator $\mathcal{G}$ provides for determination of the future field distribution from its past distribution. σ is a model parameter depending on the experimental setup and will be specified in greater detail later. An arbitrary point $\mathbf{s}$ and its surroundings $\mathbf{s}' \in \mathcal{S}$ are illustrated in Fig. 1.

The source of information for modeling the field generator is a field record containing joint sample pairs $\varphi(\mathbf{s})$ and $\varphi(\mathbf{s}' \in \mathcal{S})$. These joint sample pairs form a sample vector $\mathbf{V}_i(\mathbf{s}) = (\varphi_i(\mathbf{s}), \varphi_i(\mathbf{s}' \in \mathcal{S}))$. To make further derivation more transparent, the past field distribution $\varphi_i(\mathbf{s}')$ and the future field distribution $\varphi_i(\mathbf{s})$ will be denoted by $\mathbf{x}_i$ and $\mathbf{y}_i$, respectively. Hence $\mathbf{V}_i(\mathbf{s}) = (\mathbf{y}_i, \mathbf{x}_i)$.

The samples $\mathbf{V}_i$ are interpreted as random variables and can therefore be used to express the *joint probability distribution function* (PDF) by the kernel estimator [15]

$$f_N(\mathbf{V}) = \frac{1}{N}\sum_{i=1}^{N}\psi(\mathbf{V} - \mathbf{V}_i, \sigma), \tag{2}$$

in which ψ denotes an acceptable kernel function such as the Gaussian function $\psi(x - x_i, \sigma) = 1/(\sqrt{2\pi}\sigma)\exp(-(x - x_i)^2/2\sigma)$ and N is the number of sample pairs.

Once the samples from the field record have been taken, the question of *how to determine the optimal predictor*

becomes relevant. We consider as an optimal predictor of the future field distribution $\mathbf{y}$ from a given value $\mathbf{x}$ the value $\hat{\mathbf{y}}$ at which the mean square prediction error is minimal:

$$\mathrm{E}[(\mathbf{y}-\hat{\mathbf{y}})^2|x] = \min(\hat{\mathbf{y}}). \quad (3)$$

Here $\mathrm{E}[\,]$ denotes averaging over all points in a field record at a given time t. The solution of Eq. (3) yields together with PDF from Eq. (2) *the conditional average estimator*

$$\hat{\mathbf{y}}(\mathbf{x}) = \frac{\sum_{i=1}^{N} \mathbf{y}_i \psi(\mathbf{x}-\mathbf{x}_i,\sigma)}{\sum_{j=1}^{N} \psi(\mathbf{x}-\mathbf{x}_j,\sigma)} = \sum_{i=1}^{N} \mathbf{y}_i C_i(\mathbf{x}), \quad (4)$$

where coefficients of the expansion $C_i(\mathbf{x})$ represent basis functions that measure the similarity between the temporary vector $\mathbf{x}$ and vector $\mathbf{x}_i$ from the field record. The conditional average estimator described by Eq. 4 represents a radial basis function neural network in which the recorded data $\mathbf{x}_i, \mathbf{y}_i$ represent the memorized contents of neurons, $\mathbf{x}$ and $\hat{\mathbf{y}}(\mathbf{x})$ are the input and the output of the network, while the basis functions $C_i(\mathbf{x})$ correspond to activation functions of neurons. Since $\sum_{i=1}^{N} C_i(\mathbf{x}) = 1$, the conditional average estimator represents a normalized radial basis function neural network.

2.2 Quality of predictor

Working towards optimal modeling of future field distributions requires a quantitative estimation of modeling quality. We therefore introduce *a testing field* $\mathbf{y}$ and define the *prediction quality* Q, based upon the difference between the predicted field $\hat{\mathbf{y}}$ and the testing field $\mathbf{y}$ as:

$$Q = 1 - \frac{\mathrm{E}[(\hat{\mathbf{y}}-\mathbf{y})^2]}{\mathrm{E}[(\hat{\mathbf{y}}-\hat{\bar{\mathbf{y}}})^2] + \mathrm{E}[(\mathbf{y}-\bar{\mathbf{y}})^2]}. \quad (5)$$

Here $\hat{\bar{\mathbf{y}}}$ and $\bar{\mathbf{y}}$ stand for the average values of predicted field $\hat{\mathbf{y}}$ and testing field $\mathbf{y}$, *i.e.*, $\mathrm{E}[\hat{\mathbf{y}}] = \hat{\bar{\mathbf{y}}}$ and $\mathrm{E}[\mathbf{y}] = \bar{\mathbf{y}}$. A perfect prediction $\hat{\mathbf{y}} = \mathbf{y}$ yields $Q = 1$, while uncorrelated $\hat{\mathbf{y}}$ and $\mathbf{y}$ with equal mean values $\bar{\mathbf{y}} = \hat{\bar{\mathbf{y}}}$ result in $Q = 0$.

2.3 Prediction of field evolution

The prediction process consists of three steps:

1. *Learning*, that corresponds to *setting up the basis of joint sample pairs* $(\varphi_i(\mathbf{s}), \varphi_i(\mathbf{s}' \in \mathcal{S}))$ = $(\mathbf{x}_i, \mathbf{y}_i)$ from the field record,
2. *predicting the field* $\hat{\mathbf{y}}$ by using the conditional average estimator from Eq. (4),
3. and, if the testing field exists, *comparing predicted field with testing field* and calculating prediction quality Q.

In order to achieve the highest quality of prediction for the process, answer to the following crucial question is needed:

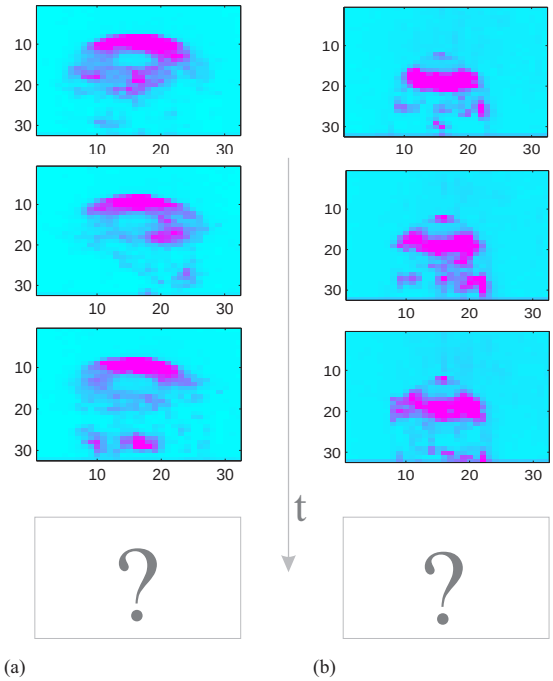

(a) (b)

Fig. 2 Time series of laser welding records for two different welding regimes: (a) a deep welding regime , and (b) a heat conduction welding regime. The next time-step images denoted by *?* are unknown and must be predicted.

- How to find the surrounding $\mathcal{S}$ of a given point $\mathbf{s}$, which gives the best prediction of field $\hat{\varphi}(\mathbf{s})$ at this point?

This question will be addressed in the following chapters.

3 Time evolution of melt pool

Characteristic dynamic properties of laser welding process in space and time can be experimentally obtained by recording the surface optical activity of the melt pool. With respect to the energy supplied to the material, various dynamic regimes of the welding process can be distinguished. In Fig. 2 visual records of two different welding regimes are shown, a deep welding regime (a) and a heat conduction welding regime (b). The deep welding regime results in a higher quality weld than the heat conduction welding regime. In the following discussion, only the deep welding regime is considered.

Dynamics of the welding regime are here represented by a record of 1000 images of size 32×32 points in space with sampling time 1/220 s. This experimental record forms a three-dimensional field of light intensity $\varphi(\mathbf{s} = \mathbf{r}, t)$ in two-dimensional space $\{(r_{x,i}, r_{y,i}); i = 1,..32, j = 1..32\}$ and time $\{t_k; k = 1..1000\}$. Due to local energy supply, the field is non-homogeneous in space. Consequently, we model its evolution locally at each spatial point separately. A model of field evolu-

tion, *i.e.*, the *learning sample* is formed from the first 800 images. We then predict the time evolution of the field and compare it with the next 200 images, which represent the *testing sample*. Based on the quality Q of these predicted images, we optimize our prediction procedure, *i.e.*, and define the structure of the surroundings $\mathcal{S}$.

3.1 Optimizing model structure

Our next goal is to find an optimal structure of radial basis function neural network which yields the best quality of prediction in the shortest time interval. The structure of surrounding set $\mathcal{S}$ plays an important role in this optimization process since each additional point in the surrounding increases the dimensionality of vectors $\mathbf{x}_i$ and therefore the time needed to predict the field distribution in a given point. Our task is to find the smallest surrounding of point $\mathbf{s}$, which results in high prediction quality.

In Fig. 3 the prediction quality is presented for various selections of surrounding set $\mathcal{S}$. Our model structure consisted of N=600 sample pairs, parameter σ was set to 4. Q represents the average quality of ten predicted images which were compared with the corresponding images from the testing field. All the member points of the first six surrounding sets in the diagram lie in the plane t_{-1}. Member points of other surrounding sets lie in several planes. For each of these, only those planes containing the member points are plotted.

As can be seen in Fig. 3, the smallest surrounding sets give the best quality of prediction - see sets Nr. 1-3 and 7-10. If more points belonging to the same time-plane are added to $\mathcal{S}$, prediction quality is decreased- compare, for example sets Nr. 1 and Nr. 6 or Nr. 14 and Nr. 15. In contrast, surrounding sets containing points from two planes, t_{-1} and t_{-2}, give a slightly better Q than sets containing only points from t_{-1} - compare for example sets Nr. 1 and Nr. 7. However, an addition of multiple time-planes reduces the quality (see set Nr. 12).

As the best quality is obtained for set Nr. 7, this surrounding set is considered optimal in further calculations. We would like to stress, that in Fig. 3 only those surrounding sets which seemed to have the potential to give the best quality were taken into account. The optimal structure of $\mathcal{S}$ was chosen on the basis of selected sets. To be sure that the chosen structure was really optimal, it is necessary to calculate the prediction quality of all the subsets containing all combinations of neighboring points. Since the number of points in our learning set is $32\times32\times600$, a calculation of Q for all sets would become a computationally prohibitive task.

3.2 Optimal prediction of melt pool evolution

Using the optimal structure of our model, we show the discrepancy between the predicted images of the laser welding melt pool and the corresponding images from the testing field. In Fig. 4 we present predicted laser welding image and corresponding image from the testing field for the optimal model structure. The surrounding set $\mathcal{S}$ has only two member points, both having the same spatial position as the predicted point, but neighboring positions in time. $N = 600$ sample pairs are taken into acount, parameter σ is set to 4. Since the quality of prediction is 0.93 (see Fig. 3), a very good similarity between the predicted and corresponding image from the testing field is expected. Comparison of predicted image and image from the testing field in Fig. 4 indeed exhibits a good resemblance. However, we would like to draw attention to surface smoothness. As can be seen, the predicted surface is smoother than the original surface. This can be easily understood if the origin of prediction of images in the conditional average estimator (Eq. 4) is taken into account. Predicted $\hat{\mathbf{y}}$ is therefore a weighted average of all those $\mathbf{y}_i$, for which $\mathbf{x}_i$ is similar to $\mathbf{x}$. Consequently, the surface roughness is diminished due to conditional averaging.

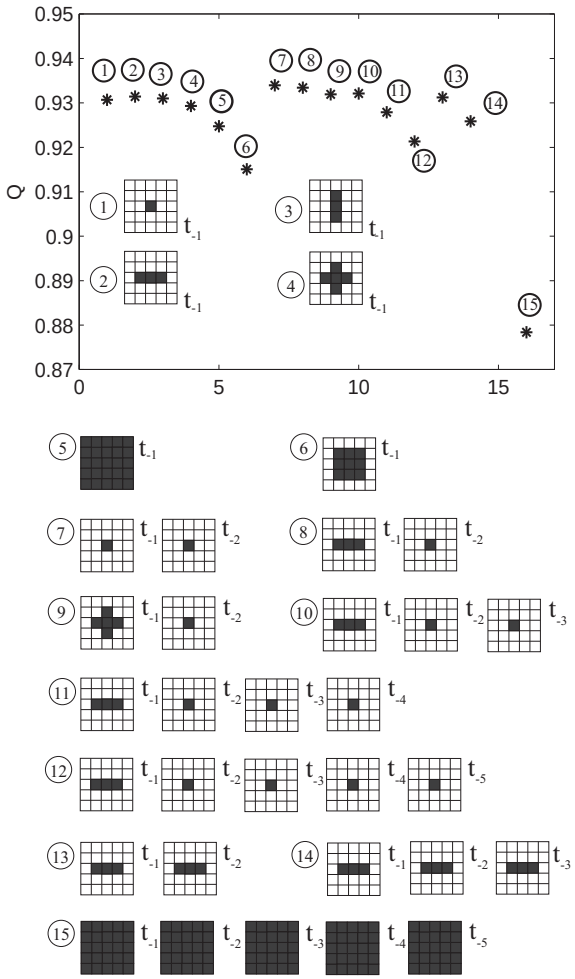

Fig. 3 Dependence of prediction quality Q (*) on the structure of the surrounding set $\mathcal{S}$, $\mathbf{s}' \in \mathcal{S}(\mathbf{s})$. Model structure consisted of $N = 600$ sample pairs, σ was set to 4. The black squares in the netlike patterns (1-15) describe the position of surrounding points. Only those time planes are plotted, which contain points from $\mathcal{S}$.

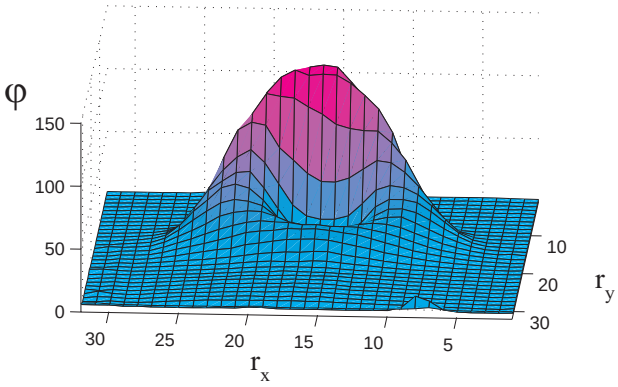

a) predicted field

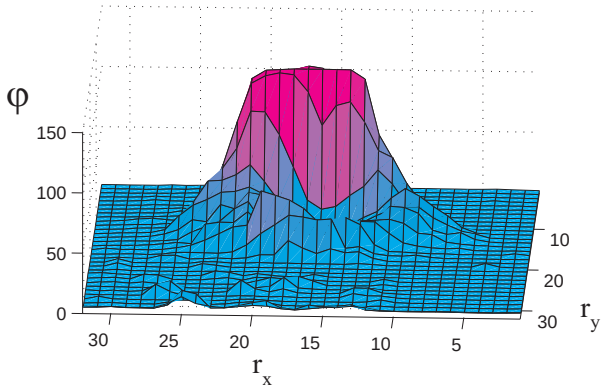

b) testing field

Fig. 4 Comparison of predicted melt pool image (a) with corresponding image from the testing field (b) for a randomly chosen testing record. φ stands for field, r_x and r_y denote spatial coordinates of the record. Parameters are $N = 600$ and $\sigma = 4$. The surrounding set $\mathcal{S}$ has only two member points, both having the same spatial position ($\mathbf{r}$) as the predicted point $\mathbf{s}$=($\mathbf{r}$,t), but different neighboring positions in time, *i.e.*, t_{-1} and t_{-2}.

4 Conclusion

Time evolution of multi-dimensional fields is usually obtained by solving a system of partial differential equations. However, if the only source of information is a record of the field, a neural network can successfully replace differential equations by extracting field evolution properties from the recorded data [16]. Neural-network-like structures are also expected to be the working algorithm of living organisms' intelligence. In the same way as neural networks, living organisms predict the evolution of events in their surroundings solely on the basis of recorded data. It could be conjectured that this operation is probably performed by extracting simple evolution laws from recorded data.

In this paper we show how to optimize a statistical modeling of a field generator performed by the normalized radial basis function neural network, to efficiently learn spatiotemporal dynamics of multi-dimensional fields. In our experimental approach, all information about process dynamics is contained in a measured space-time record of the characteristic variable. To extract the model of field evolution from the corresponding discrete sample data, we employ a non-parametric approach, following a state-space reconstruction technique. The basis of state-space reconstruction is the formation of sample vectors which are composed of past and future field distributions. We assume that the field distribution in a given spatiotemporal point $\mathbf{s}$ is correlated with the field distribution in the spatiotemporal surroundings of this point, $\mathcal{S}$. The prediction of field distribution in $\mathbf{s}$ is then accomplished as a mapping relation between the field distribution in the surroundings $\mathcal{S}$ and field distribution in $\mathbf{s}$.

Since the optimization of the state-space reconstruction technique also requires a quantitative measure of the prediction quality, we introduce the quality estimator Q, which incorporates the difference between the predicted field and the corresponding testing field. We consider as a proper set of model parameters those values at which the prediction quality achieves a maximum. This strategy is used here to find a proper value of parameter σ and the structure of the surrounding $\mathcal{S}$ utilized in the prediction process. Generally, an estimation of the proper number of sample points must also consider the complexity of the experiments, which is numerically demanding in a multidimensional case [17].

We demonstrate the proposed method of modeling of the properties of the laser-heated melt pool. For this purpose, we employ non-parametric statistical modeling of field evolution on a spatiotemporal record of the melt pool of the laser welding process. The major part of the field record is used for learning, while the minor part of the record serves for testing. We show how to construct the set of joint sample pairs containing past and future values of field distributions and pay special attention to the structure of these sample pairs. We also present the optimal structure of sample vectors, which gives the highest resemblance between predicted images and images from the testing field and has a small number of member points in order to make the prediction algorithm work quickly.

5 References

[1] E. Govekar, J. Gradišek, I. Grabec, M. Geisel, A. Otto, M. Geiger, "On characterization of CO_2 laser welding process by means of light emitted by plasma and images weld pool", in *Third Int. Symp: Investigation of Non-linear Dynamics Effects in Production Systems* (Cottbus, Germany), 2000.

[2] E. Govekar, J. Gradišek, I. Grabec, M. Geisel, A. Otto, M. Geiger, "Influence of feed rate on dynamics of laser welding process" in *Second Int. Symp: Investigation of Non-linear Dynamics Effects in Production Systems* (Aachen, Germany), 1999.

[3] M. Casdagli, S. Eubank, "Nonlinear Modeling and Forcasting", Santa Fe Institute: Addison-Wesley,

1992.

[4] H. D. I. Abarbanel, R. Brown, J. J. Sidorowich, L. S.Tsmiring, ”The analysis of observed chaotic data in physical systems”,*Rev. Mod. Phys.* Vol. 65, pp.1331-1392, 1993.

[5] E. J. Kosterlich, T. Schreiber, ”Noise reduction in chaotic time-series data: A survey to common methods ”,*Phys. Rev. E* Vol. 48, pp.1752-1763, 1993.

[6] H. Kantz, T. Schreiber, ”Nonlinear Time Series Analysis”, Cambridge University Press, 1997.

[7] S. Sigert, R. Friedrich, J. Peinke, ”Analysis of data sets of stochasitc systems”, *Phys. Lett. A* Vol. 243, pp.275-289, 1998.

[8] D. M. Rubin, ”Use of forecasting signatures to hlep destinguish preiodicity, randomness, and chaos in ripples and other spatial patterns”, *Chaos* Vol. 2, pp.525-535, 1992.

[9] I. Grabec, S. Mandelj, ”Continuation of chaotic fields by RBFNN”, in *Biological and Artificial Computation: From Neuroscience to Technology: Proc.*, eds. J. Mira, R. Moreno-Diaz, J. Cebestany, Lecture Notes in Computer Science (Springer-Verlag, Berlin), Vol. 1240, pp.597-606, 1997.

[10] S. Ørstavik, J. Stark, ”Reconstruction and cross-prediction in coupled map lattices using spatiotemporal embedding techniques”, *Phys. Lett. A* Vol. 247, pp.145-160, 1998.

[11] U. Parlitz, C. Merkwirth, ”Prediction of spatiotemporal time series based on reconstructed local states”, *Phys. Rev. Lett.* Vol. 84, pp.1890-1893, 2000.

[12] S. Mandelj, I. Grabec and E. Govekar, ”Statistical modeling of stochastic surface profiles”, *CIRP-J. Manuf. Syst*, Vol. 30, pp 281-287, 2000.

[13] S. Mandelj, I. Grabec and E. Govekar, ”Nonparametric statistical modeling of spatiotemporal dynamics based on recorded data”, *Int. Jour. Bifur. Chaos*, Vol. 14, No. 6, pp 2011-2025, 2004.

[14] A. B. Bračič, I. Grabec, E. Govekar, ”Modeling the field of laser welding melt pool by RBFNN”, *DCDIS A Supplement, Advances in Neural Networks*, Vol. 14(S1), pp 227-331, 2007.

[15] R. O. Duda, P. E. Hart, ”Pattern Clasification and Scene analysis”, J. Wiley and Sons, New York, Chap. 4. 1997.

[16] L. Ljung , ”System Identification - Theory for the User (second edition)”, Prentice-Hall, New Jersey, 1999.

[17] I. Grabec, ”Extraction of Physical Laws from Joint Experimental Data,” *Eur. Phys. J. B*, vol. 48, pp. 279-289, 2005.